

Article

Exploring the Solubility of Ethylene Carbonate in Supercritical Carbon Dioxide: A Pathway for Sustainable Electrolyte Recycling from Li-Ion Batteries

Nils Zachmann *, Claude Cicconardi and Burçak Ebin *

Department of Chemistry and Chemical Engineering, Chalmers University of Technology, Kemivägen 4, SE-412 96 Gothenburg, Sweden

* Correspondence: zachmann@chalmers.se (N.Z.); burcak@chalmers.se (B.E.)

Abstract: Ethylene carbonate is, among other applications, used in Li-ion batteries as an electrolyte solvent to dissociate Li-salt. Supercritical CO₂ extraction is a promising method for the recycling of electrolyte solvents from spent batteries. To design an extraction process, knowledge of the solute solubility is essential. In this work, the solubility of ethylene carbonate at different pressure (80–160 bar) and temperature (40 °C, and 60 °C) conditions is studied. It is shown that the solubility of ethylene carbonate increased with pressure at both temperatures, ranging from 0.24 to 8.35 g/kg CO₂. The retrieved solubility data were fitted using the Chrastil model, and the average equilibrium association number was determined to be 4.46 and 4.02 at 40 °C and 60 °C, respectively. Scanning electron microscopy, Fourier-transform infrared spectroscopy, and X-ray diffraction analysis of the collected ethylene carbonate indicated that the crystal morphology and structure remained unchanged. A proof-of-principle experiment showed that EC can be successfully extracted from Li-ion battery waste at 140 bar and 40 °C.



Academic Editors: Chiara Ferrara and Elza Bontempi

Received: 27 January 2025

Revised: 27 February 2025

Accepted: 28 February 2025

Published: 4 March 2025

Citation: Zachmann, N.; Cicconardi, C.; Ebin, B. Exploring the Solubility of Ethylene Carbonate in Supercritical Carbon Dioxide: A Pathway for Sustainable Electrolyte Recycling from Li-Ion Batteries. *Batteries* **2025**, *11*, 98.

<https://doi.org/10.3390/batteries11030098>

Copyright: © 2025 by the authors. Licensee MDPI, Basel, Switzerland. This article is an open access article distributed under the terms and conditions of the Creative Commons Attribution (CC BY) license (<https://creativecommons.org/licenses/by/4.0/>).

Keywords: supercritical CO₂ extraction; solubility; Li-ion battery electrolyte; ethylene carbonate

1. Introduction

Ethylene carbonate (EC) is a polar solvent with a dielectric constant of 89.8 at 25 °C, a dipole moment of 4.61D, and a melting point of 36.5 °C [1]. EC is used as a plasticizer, crosslinking agent, additive for lubricants, and as a (co-)solvent in the pharmaceutical industry. Moreover, EC is used in cleaning agents, agrochemicals, polymer processing, and as a functional fluid [2]. The biggest global market share for EC in the industry is its application as an electrolyte solvent in Li-ion batteries [3,4]. The electrolyte in Li-ion batteries is typically a mixture of polar (i.e., EC, propylene carbonate) and non-polar (i.e., dimethyl carbonate, ethyl methyl carbonate, and diethyl carbonate) solvents to dissociate the conductive salt while maintaining low viscosity [3]. The recycling of the electrolyte from spent Li-ion batteries remains a challenge for the Li-ion battery industry [5]. Literature suggests different approaches to recover the electrolyte from spent LIBs. Among them are vaporization processes, organic solvent extraction, and supercritical CO₂ (scCO₂) extraction [5–9]. The drawback of vaporization processes is that the conductive salt, LiPF₆, decomposes to toxic gases such as hydrofluoric acid and organo-fluorophosphates [10].

ScCO₂ extraction has high potential to recover the electrolyte [5,7]. Compared to conventional extraction techniques, scCO₂ extraction is superior in terms of sustainability aspects as CO₂ is non-toxic, non-carcinogenic, non-flammable, thermodynamically stable,

abundant, and can be recycled back into the process [11]. Moreover, it possesses excellent mass transfer characteristics owed to its liquid-like densities, gas-like viscosities, negligible surface tension, and high diffusion coefficient [12]. Any contamination of the sample matrix during the extraction process is suppressed in scCO₂ extraction processes as the solvent can be quickly removed by depressurization. Another advantage is that CO₂ can be regenerated into the process after separation from the solute [11]. The solvent characteristics of scCO₂ can be easily fine-tuned by changing pressure or temperature conditions. Generally, an increase in pressure at a given temperature leads to an increase in solvent density, by which the solvent power increases as the probability of solvent–solute interactions increases. The effect of temperature at a given pressure is somewhat more complex, and its tendency is dependent on the cross-over pressure. Below the cross-over pressure, the solvation power decreases with an increase in the temperature due to the solvent density decrease. Above the cross-over pressure, the density effects become less dominant as the solvent changes are no longer remarkable, and solute vapor pressure effects become dominant. Consequently, the solubility increases with temperature [12,13].

ScCO₂ is classified as a non-dipolar solvent and is thus effective in dissolving non-polar, low-molecular-weight compounds. Literature shows that non-polar electrolyte solvents were successfully extracted using scCO₂ [14,15]. EC is more challenging to be extracted in scCO₂ due to its high polarity. However, EC contains a CO₂-philic carbonyl group, which improves the solvation of polar compounds in scCO₂ [16,17]. Knowledge of the solute solubility is a key factor in designing an extraction process as the extraction rate of a solute from a certain matrix is governed by the solubility and mass-transfer, i.e., partitioning and diffusion [18,19]. The process conditions leading to high solubility can be used for the extraction of the solute, and the low-solubility conditions can be then used for the separation of the extracted substance from the CO₂ [11]. A study investigated the solubility of CO₂ in EC at different temperatures (18–58 °C) at atmospheric pressure and reported a decrease in the CO₂ mole fraction with temperature from 0.00622 to 0.00274 [20]. However, there is a lack of phase equilibria data or solubility data for EC in scCO₂ conditions in the literature.

In this work, the solubility of EC in scCO₂ at different pressure conditions (80 to 160 bar) at isothermal temperatures (40 °C and 60°) was studied. The retrieved solubility data of EC in scCO₂ will be a key factor in the design of a scCO₂ extraction process to recover the electrolyte from spent Li-ion batteries.

2. Materials and Methods

2.1. Materials

Liquid carbon dioxide (CO₂) with a purity of ≥99.99% (H₂O ≤ 5 ppm *w/w*) was purchased from Air Liquide (Paris, France). Ethylene carbonate (>98%) was purchased from Merck Millipore.

2.2. Experimental

The solubility of EC in supercritical CO₂ was isothermally (40 °C and 60 °C) determined at different pressure conditions (80 to 160 bar) using the gravimetric flow-through method. Thereby, the equilibrium chamber was loaded with an adequate amount of solute. ScCO₂ is passed from top to bottom in a continuous flow, and the solubilized solute is trapped in the collection vial by reducing the pressure. The solubility was then determined using the weight of the trapped amount and the total mass of passed CO₂ [21].

The experimental set-up is illustrated in Figure 1. Pure EC (1.00 ± 0.05 g) was placed inside a stainless-steel equilibrium chamber (7.5 mL), which was leak-tight closed using wrenches. The equilibrium chamber was then thermally stabilized to the desired temper-

ature using water pipes connected to an external water bath (Model F12 & ED; Julabo, Seelbach, Germany). The temperature in the equilibrium chamber was monitored using a thermocouple connected to a temperature logger and the pressure using a pressure gauge. The equilibrium chamber was pressurized using a syringe pump connected to a heating jacket (ISCO 260D; Teledyne ISCO, Lincoln, NE, USA), and the system was equilibrated for 7.5 min before the CO₂ flow was started. A CO₂ flow was initiated using a metering valve and was adjusted to the desired flow rate, 1500 ± 300 mL/min, which was measured at depressurized conditions at 1 bar and 22 ± 1 °C. The flowrate was adjusted to be as low as possible to achieve saturation. The effluent of the equilibrium chamber was filtered using a stainless-steel filter (0.5 µm) before passing through the metering valve to prevent the leak of undissolved EC. The flow was kept constant for 5 min, and the solubilized EC was collected in two successive collection vials to maximize the collection yield. After 5 min, the collection vials were weighted using a precision scale (resolution 0.01 mg and linearity ±0.1 mg), and meanwhile, the equilibrium chamber was held in static pressure for 5 min. The procedure was repeated several times until the collected EC amount approached the input weight. At all pressure and temperature conditions, the experimental runs were conducted three times.

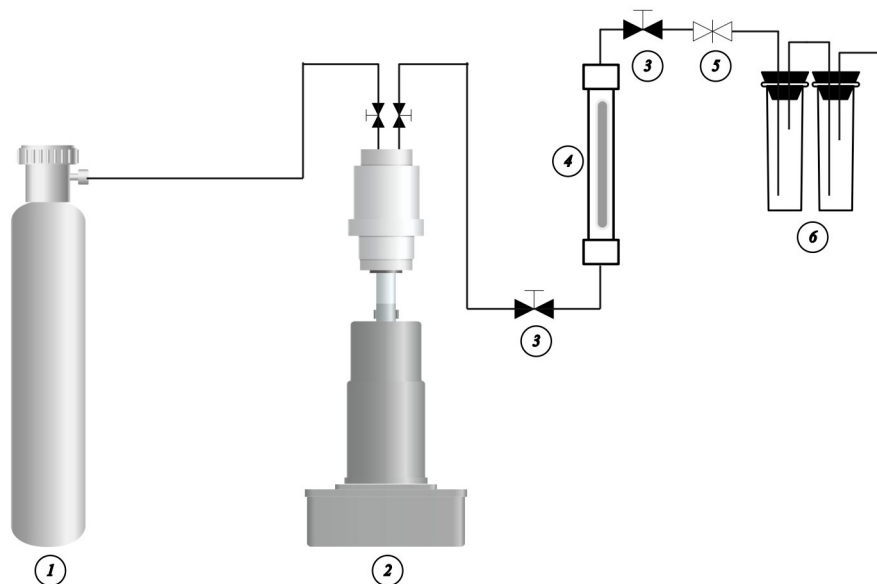


Figure 1. Schematic of the experimental set-up. (1) CO₂ tank, (2) syringe pump connected to a heating jacket, (3) on/off valve, (4) equilibrium chamber connected to a thermal couple and a pressure gauge, (5) metering valve, and (6) collection vials.

A proof-of-concept experiment was conducted to extract EC from Li-ion battery black mass. The extraction chamber was loaded with the sample (5.5 ± 0.3 g). After an equilibration time of 5 min, a constant flow of CO₂ was applied (1500 ± 300 mL/min measured at depressurized conditions, 1 bar, 22 ± 1 °C). The extracts were absorbed in a glass vial filled with acetonitrile (4 mL). Two approaches were compared. In the first approach, an extraction time of 45 min was selected using 140 bar and 40 °C. In the second approach, three subsequent extraction steps were used for the extraction of the EC from the same black mass sample. The first step involved dynamic extraction for 30 min at 80 bar and 40 °C, then the pressure was raised to 100 bar in the second extraction step for 30 min, and finally raised to 140 bar for another 30 min. Then, the extract solution was analyzed using gas chromatography coupled with mass spectrometry (GC-MS). To determine the extraction yield of EC, the content of EC in the black mass was analyzed before the scCO₂ extraction process. Therefore, a procedure developed by Peschel et al. was adopted [22].

The black mass sample (5.2 ± 0.02 g) was mixed with acetonitrile (5 mL) inside a plastic vial (50 mL). Then, the vial was shaken for 5 min, and the extraction solution was filtered. Afterward, the solution was analyzed using GC-MS.

2.3. Calculation of the Solubility and Molar Fraction Solubility

To calculate the solubility of EC in CO_2 , the cumulative collected amount of EC (g) was plotted against the amount of consumed CO_2 (g).

The solubility of EC at the corresponding scCO_2 condition was then determined using the slope coefficient of the linear regression of data points within the linear range of the extraction curve. The amount of consumed CO_2 was calculated based on the following equation (Equation (1)):

$$m = V\rho \quad (1)$$

where V is the consumed CO_2 in ml during the extraction period of 5 min given by the pressurized syringe pump at the corresponding pressure condition, and ρ is the density (g/mL) at the process condition taken from the NIST Chemistry Webbook [23]. As the CO_2 flowrate fluctuated during the extraction period of 5 min, the consumed CO_2 volume differed slightly between the serial runs.

The molar fraction solubility of EC (x_{EC}) was calculated according to Equation (2).

$$x_{\text{EC}} = S \frac{MM_{\text{CO}2}}{MM_{\text{EC}}} \quad (2)$$

where S is the determined solubility, given in g/g, MM_{EC} is the molar mass of EC (88.06 g/mol), and $MM_{\text{CO}2}$ is the molar mass of CO_2 (44.01 g/mol).

2.4. Chrastil Model

The measured solubility data were modeled using the Chrastil model, as it requires only information about the density of the supercritical CO_2 , temperature, and experimental solubility data. The semi-empirical model was derived based on the formation of a solvato complex at equilibrium between the solute and scCO_2 molecules. It relates solute solubility to temperature and the pure supercritical fluid solvent density up to a solute concentration of 200 g/L. (Equation (3)) [24].

$$S = \rho^k \exp\left(\frac{A}{T} + B\right) \quad (3)$$

where S is the solubility of the solute in kg/m³, ρ is the density of the solvent in kg/m³, and T is the operating temperature in K. A , B , and k are the adjustable model parameters and can be determined using linear regression of the experimental data by plotting the natural logarithm of S against the natural logarithm of ρ . Constant A is a function of the enthalpy of solvation (ΔH_{solv}), the enthalpy of vaporization (ΔH_{vap}), and the universal gas constant, denoted as R ($A = (\Delta H_{\text{vap}} + \Delta H_{\text{solv}})/R$). B is a function of the association number and molecular weights of the solute and supercritical fluid. k is the average equilibrium association number of the pseudo solvato-complex compound.

2.5. Measurement and Characterization

Universal attenuated total reflection Fourier-transform infrared spectroscopy (ATR-FTIR, Spectrum Two, Perkin Elmer, Hägersten, Sweden) was used to characterize the collected EC and initial EC, which served as a reference. The ATR-FTIR spectra were recorded in a range between 4000 cm^{-1} and 500 cm^{-1} , with a resolution of 2 cm^{-1} and a total of 4 scans.

X-ray diffraction analysis (XRD, Bruker D8 Discover, EIGER2R 500 K detector, Dectris, Baden, Switzerland) was performed to analyze potential structural changes of the initial and collected EC at different conditions. The pattern was recorded in a 2θ range of 10° to 55° using the characteristic K_α wavelength of 1.5406 \AA provided by a Cu radiation source. The operating voltage and current were set to 40 kV and 40 mA and the operational speed of 15 rpm. The sample preparation for the XRD measurement included grinding of the samples to approximately the same particle size (evaluated by eyesight), and then the sample holder was filled and pressed with a glass piece.

Scanning electron microscopy (SEM, Quanta 200 ESEM, FEI, Lausanne, Switzerland) with 5 kV high voltage and ETD detector was used to study the surface morphology of the samples. The collected and initial EC was placed on a graphite substrate and coated with a gold film (5 nm) using a sputter (EM ACE 600, Leica, Wetzlar, Germany).

GC-MS (GC-2030 NX, GCMS-QP2020 NX, Shimadzu, Kyoto, Japan) was used to quantitatively analyze the extract solutions. Split injection (1:20) with a purge flow of 3 mL/min was used for sample injection into the column (Zebtron ZB-5MS column, $30 \text{ m} \times 250 \mu\text{m} \times 0.25 \mu\text{m}$). The injection and transfer line temperature were set to 270°C and 230°C , respectively. Helium was used as carrier gas at a flowrate of 1 mL/min. The GC oven temperature was maintained at 40°C for 1 min and then ramped at $20^\circ\text{C}/\text{min}$ to 260°C , which was held for 2 min. MS conditions were electron impact, ionization source temperature of 230°C , 70 eV filament voltage, and mass range of 30–300 m/z . The integrated area of EC was used for quantification.

3. Results and Discussion

The solubility of EC in scCO₂ was studied at different isothermal (40°C and 60°C) pressure conditions (80, 100, 120, 140, and 160 bar). Therefore, the cumulative collected EC (g) was plotted over the CO₂ amount (g). The solubility of EC in CO₂ was determined based on the linear slope. The results at the different pressure conditions for 40°C are plotted in Figure 2. The corresponding solubility data are given in Table 1. The respective plots used for the isothermal condition at 60°C are plotted in Figure S1 in the Supplementary Material.

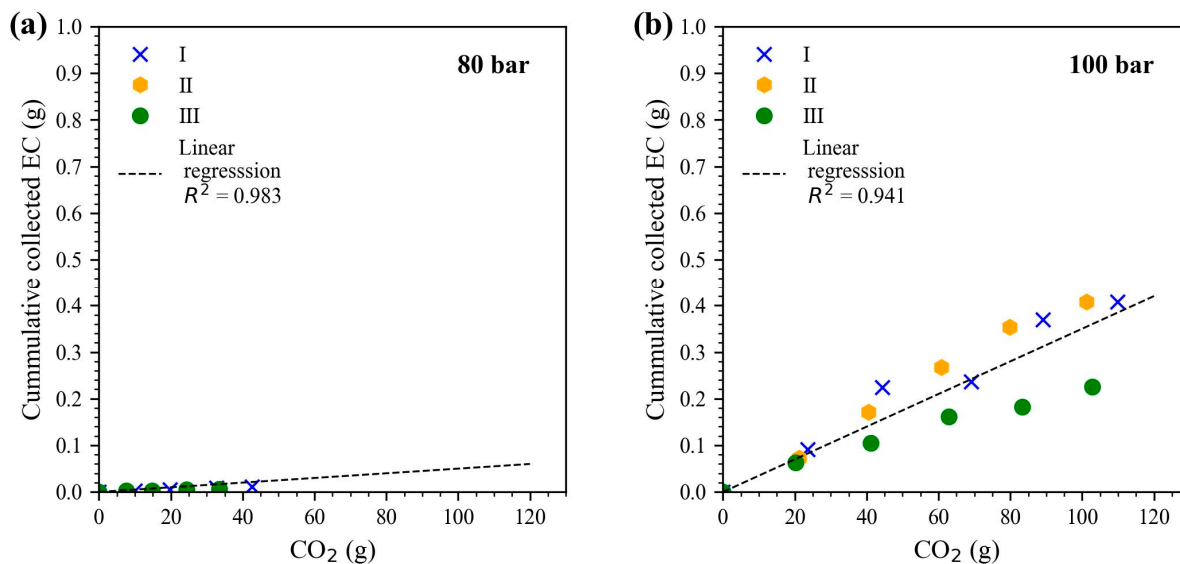


Figure 2. Cont.

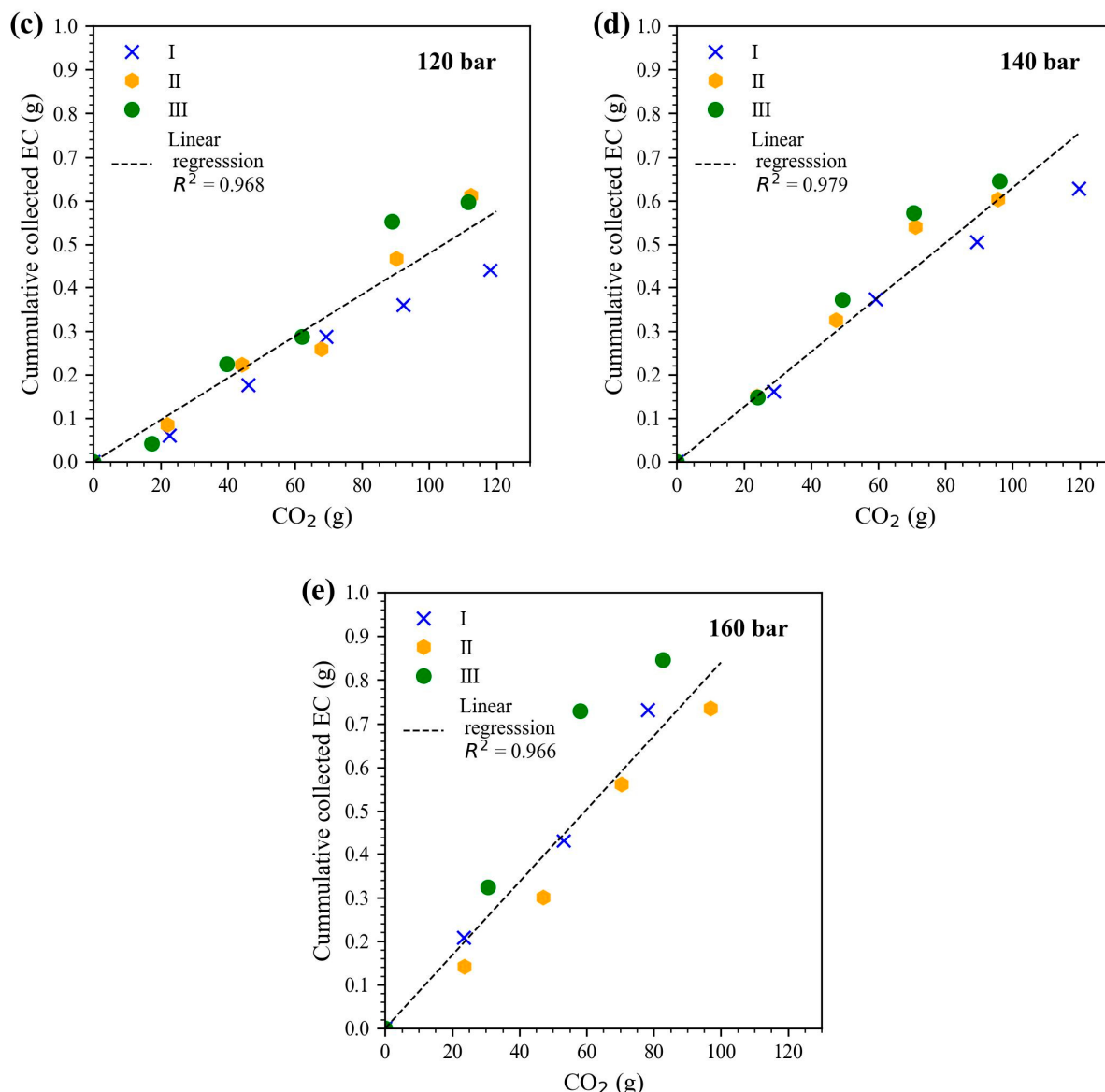


Figure 2. Cumulative collected EC (g) plotted against the CO₂ of the different experimental runs (denoted as I, II, and III) at (a) 80 bar, (b) 100 bar, (c) 120 bar, (d) 140 bar, and (e) 160 bar and isothermal conditions at 40 °C. The linear regression for the determination of the solubility is shown as a dashed line.

Table 1. Experimental solubilities of ethylene carbonate in supercritical carbon dioxide based on the results presented in Figure 2 and Figure S1. ^a Standard uncertainty of the temperature and pressure were 2 °C and 5 bar, respectively. ^b Density data were taken from the NIST Chemistry WebBook [23]. ^c Slope (g/kg CO₂) of the linear regression is shown in Figure 2 and Figure S1. ^d Uncertainties (\pm) refer to the standard error of the slope of the linear regression.

Temperature ^a (°C)	Pressure ^a (bar)	CO ₂ Density ^b (kg/m ³)	Solubility (g/kg CO ₂)	Mole Fraction Solubility ($\times 10^{-3}$)
40	80	277.9	0.24 ^c \pm 0.02 ^d	0.12
	100	628.6	3.5 \pm 0.2	1.74
	120	717.8	4.8 \pm 0.2	2.37
	140	763.3	6.4 \pm 0.3	3.17
	160	794.9	8.4 \pm 0.5	4.17

Table 1. Cont.

Temperature ^a (°C)	Pressure ^a (bar)	CO ₂ Density ^b (kg/m ³)	Solubility (g/kg CO ₂)	Mole Fraction Solubility (×10 ⁻³)
60	80	191.6	0.56 ± 0.09	0.28
	100	289.9	0.50 ± 0.03	0.25
	120	434.4	1.7 ± 0.2	0.86
	140	561.4	3.6 ± 0.3	1.78
	160	637.5	5.5 ± 0.4	2.75

The mole fraction solubility of EC in supercritical CO₂ is plotted in Figure 3. The solubility of EC in scCO₂ increases with pressure at a constant temperature in the range from 0.24 g/kg CO₂ to 8.35 g/kg CO₂. The increase in solubility under increased pressure can be linked to the increased likelihood of specific solute–solvent interactions caused by the increased density of CO₂ [12]. The solubility at 40 °C was higher than at 60 °C measured at the same pressure conditions. This indicates that the studied pressure range was below the cross-over pressure, meaning that the CO₂ density was the dominating factor in dissolving EC [12,13]. The solubility at 80 bar and 40 °C is very low compared to the solubility at 140 bar and 40 °C. Thus, for the design of an extraction process for EC recycling, 140 bar and 40 °C can be used for the extraction of the solute, while the low solubility condition at 80 bar and 40 °C can be used for the separation of the extracted substance from the CO₂ [11].

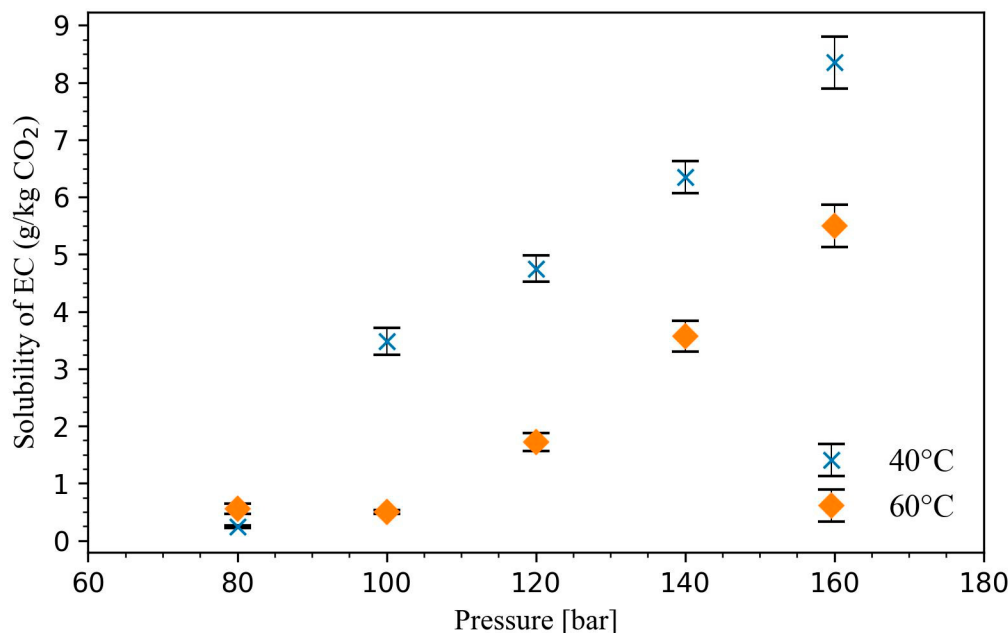


Figure 3. Solubility of EC in scCO₂ at different pressure (80, 100, 120, 140 bar, and 160 bar) at isothermal temperature (40 °C and 60 °C) conditions. The uncertainty bars represent the standard error of the linear regression slope coefficient.

As there is a lack in the literature of solubility data of EC in scCO₂, the mole fraction solubility was compared to propylene carbonate (PC) in CO₂. PC is another cyclic carbonate used in Li-ion batteries. The vapor phase composition and the calculated corresponding mole fraction solubility values reported by Hongling et al. and Rubin et al. are presented in Table S1 in the Supplementary Material [25,26]. It can be observed that the mole fraction solubility of PC in CO₂ is a magnitude higher compared to EC at similar pressure and temperature conditions. It is believed that the higher solubility of PC in CO₂ is due to its lower polarity. The vapor phase fraction reported by Hongling et al. fluctuated in the pressure range between 20 bar and 130 bar. Thus, a clear trend in terms of pressure and

temperature cannot be observed. However, according to the study by Rubin et al., the mole fraction solubility decreases with raising temperature, which was also observed for EC.

The experimental solubility data fitted well to the Chrastil model, as seen in Figure 4, and the fitting parameters are presented in Table 2. The average equilibrium association number of the pseudo solvato-complex compound determined from the Chrastil model is quite similar for 40 °C and 60 °C, at 4.28 and 4.02, respectively. This indicates that, on average, four CO₂ molecules are used to dissolve one molecule of EC. The CO₂ molecule was reported to form stable Lewis acid–Lewis base interactions with the CO₂-philic carbonyl oxygen in other esters [16]. The constant A is a magnitude higher at 60 °C compared to 40 °C, suggesting a higher solvation and vaporization enthalpy.

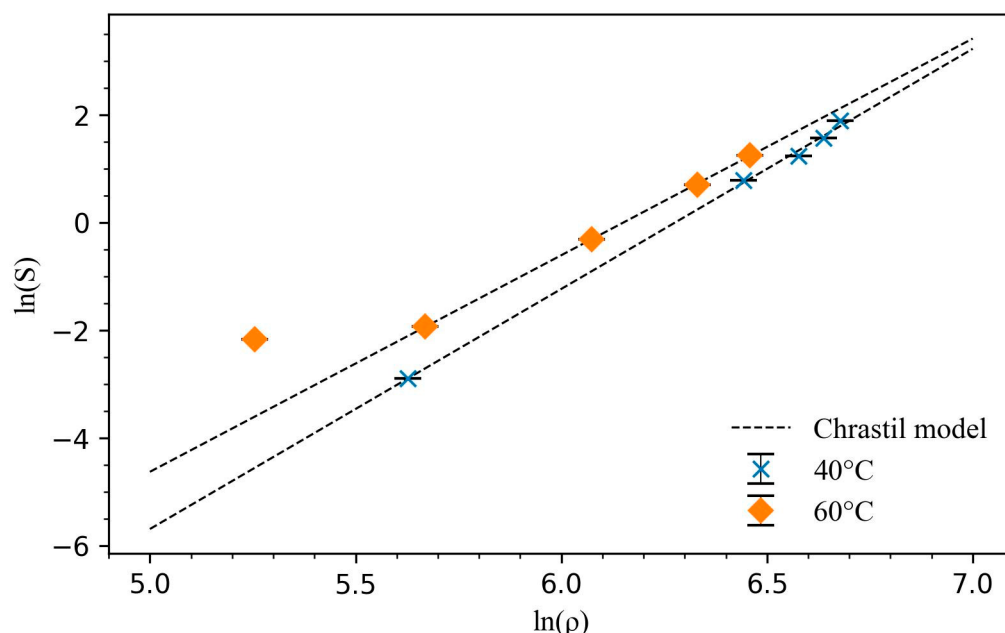


Figure 4. Correlation between the experimental and correlated solubility data using the Chrastil model.

Table 2. Fitting parameters obtained for the Chrastil equation and the R² value of the fit.

Temperature (°C)	A	B	k	R ²
40	84,329.63	-296.11	4.28	0.9992
60	506,275.19	-1544.37	4.02	0.9998

The collected EC was analyzed using FTIR to study any compositional change occurring after the scCO₂ dissolution. Figure 5 shows the spectra between 4000 and 500 cm⁻¹ at the different pressure and temperature conditions and the initial EC as a reference. The initial EC spectra match the collected EC sample without any clear peak shifts. Thus, it can be concluded that the scCO₂ extraction at the studied conditions did not affect the chemical bonding of the molecule.

XRD analysis results are plotted in Figure 6. The overlap of the peak position of the initial EC and the collected EC, which represent recovered material, indicates that the monoclinic crystal structure is stable during the processing and, generally, independent from the pressure and temperature conditions. However, random selective orientation of the crystal planes is observable in respect to the different peak intensities and shapes. The random crystal orientation may arise from the XRD sample preparation or the recrystallization process after dissolution in EC. The crystal orientation during the recrystallization process can be altered by several factors such as nucleation, growth rates, solution concentration, pre-and post-expansion pressure, and temperature [27].

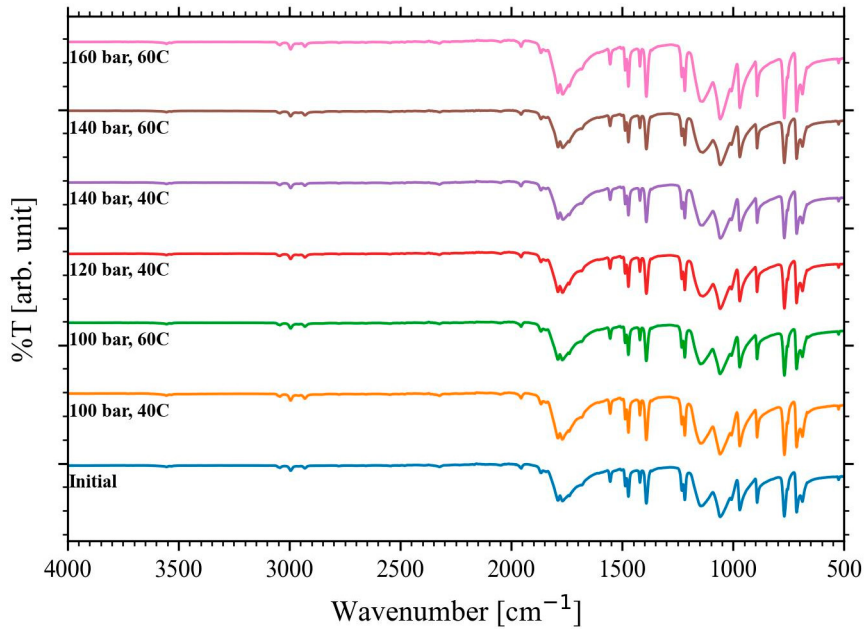


Figure 5. FTIR spectra of the scCO₂ dissolved EC and initial EC between 4000 and 500 cm⁻¹.

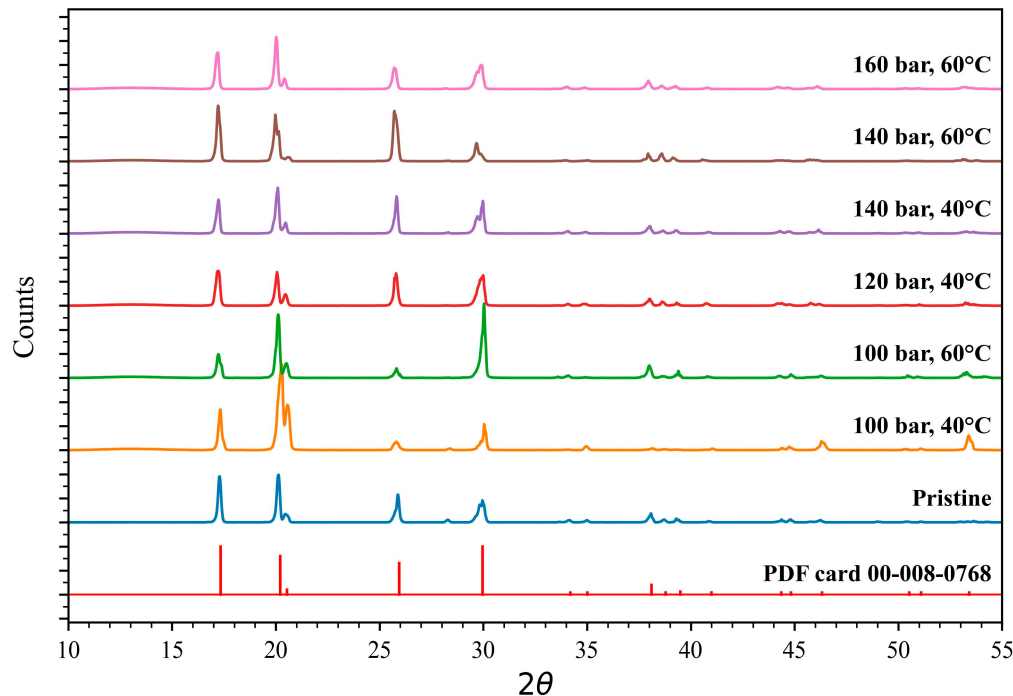


Figure 6. XRD pattern of the scCO₂ dissolved EC and the initial EC at different pressures and temperatures in the 2θ range from 10° to 55°. As a reference, the PDF card taken from EC is plotted.

ScCO₂ can be applied in micronization processes to produce powder and composites while controlling their morphology and particle size distribution [28]. The properties of the obtained product depend on the phase equilibria, thermodynamic behavior of the system, fluid dynamics, mass transfer, and nucleation growth kinetics [11]. The particle size of the collected EC appeared to be smaller than the initial EC observed by eyesight. Determination of the changes in particle diameter and particle size distribution after EC collection was not part of this study. However, micronization of the EC due to the rapid expansion of the effluent in the collection process used in the RESS process (the rapid expansion of supercritical solutions) can be expected [29]. SEM images were taken from the

initial EC and the collected EC at 140 bar and 40 °C and are given in Figure 7. According to the SEM images, the EC morphology of EC was not altered during the process. Similar findings were observed by Yim et al., as they dissolved polyvinylidene fluoride, which is a common binder for Li-ion batteries [30].

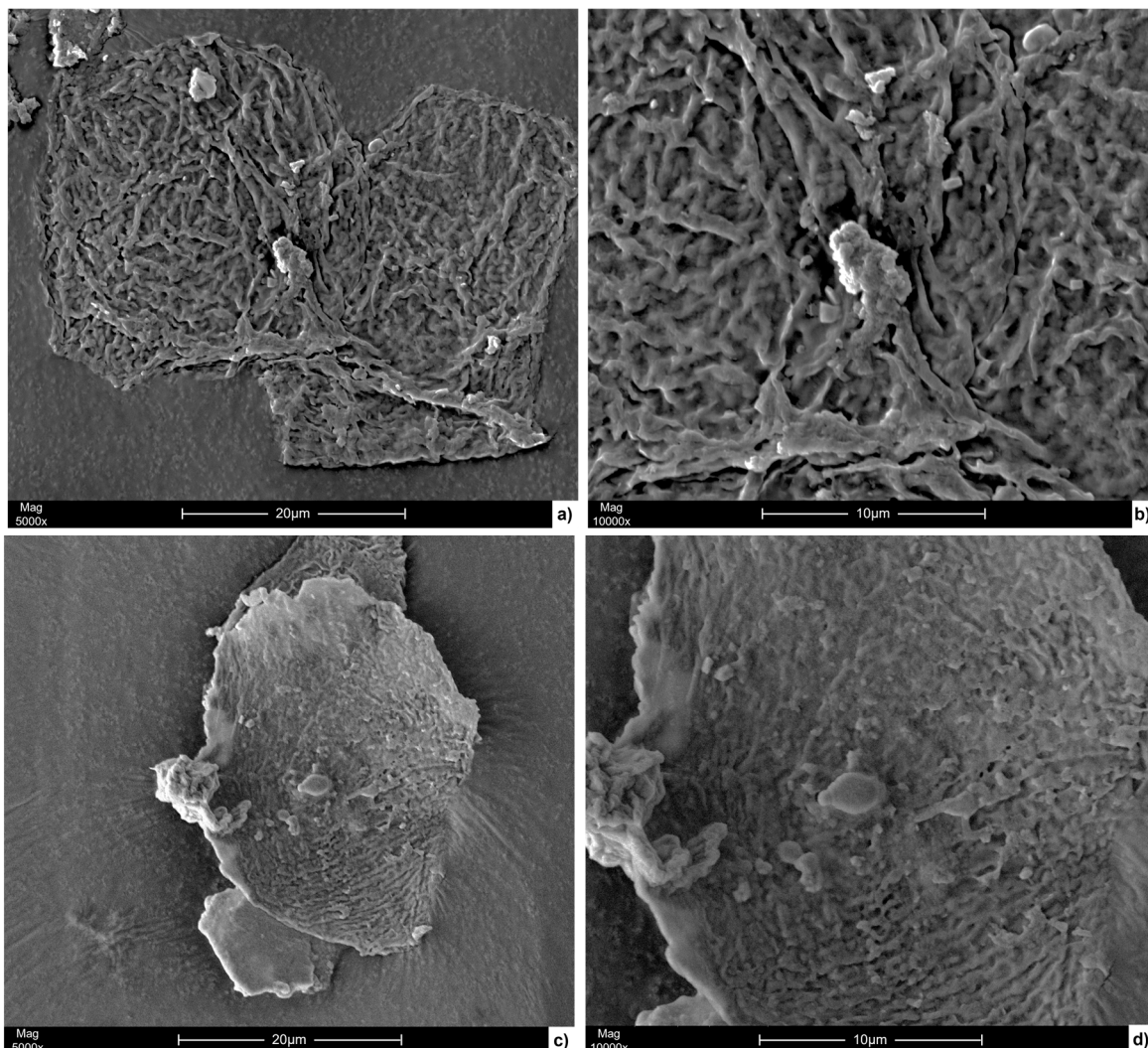


Figure 7. SEM images of the pristine EC with magnification at (a) 5000× and (b) 10,000×, as well as scCO₂ dissolved EC at 140 bar and 40 °C with magnification at (c) 5000× and (d) 10,000×.

In a previous research study, the non-polar electrolyte solvents dimethyl carbonate and ethyl methyl carbonate were selectively extracted from Li-ion battery pouch cells using different pressures (60 to 120 bar) and temperature conditions (29 °C), while EC remained in the LiB electrode stack [14]. An experiment was conducted to validate that EC can be successfully recovered from LiB waste material. Therefore, two approaches were used. In the first approach, dynamic scCO₂ extraction at 140 bar and 40 °C was applied for 45 min to extract the residual electrolyte in industrial Li-ion battery black mass. In the second approach, three subsequent steps were used for the extraction of the EC. First, the electrolyte was extracted for 30 min at 80 bar and 40 °C. The pressure was raised to 100 bar in the second extraction step for 30 min and finally raised to 140 bar for another 30 min using the same black mass. The result of the extraction yields for the different steps is plotted in Figure 8. It can be observed that an extraction yield of 90% was reached using approach 1. Approach 2 indicates the impact of the different solubilities on the extraction of EC from the LiB black mass. During the first step at 80 bars, the extraction yield of EC was

low, only 4.5%. The extraction yield increased to 38% by raising the pressure to 100 bar and finally exceeding 93% at 140 bar. This proves that EC can be successfully recovered from Li-ion battery waste using pure scCO₂ extraction at 140 bar and 40 °C. However, further research is required to study the mass transfer characteristics during the extraction process.

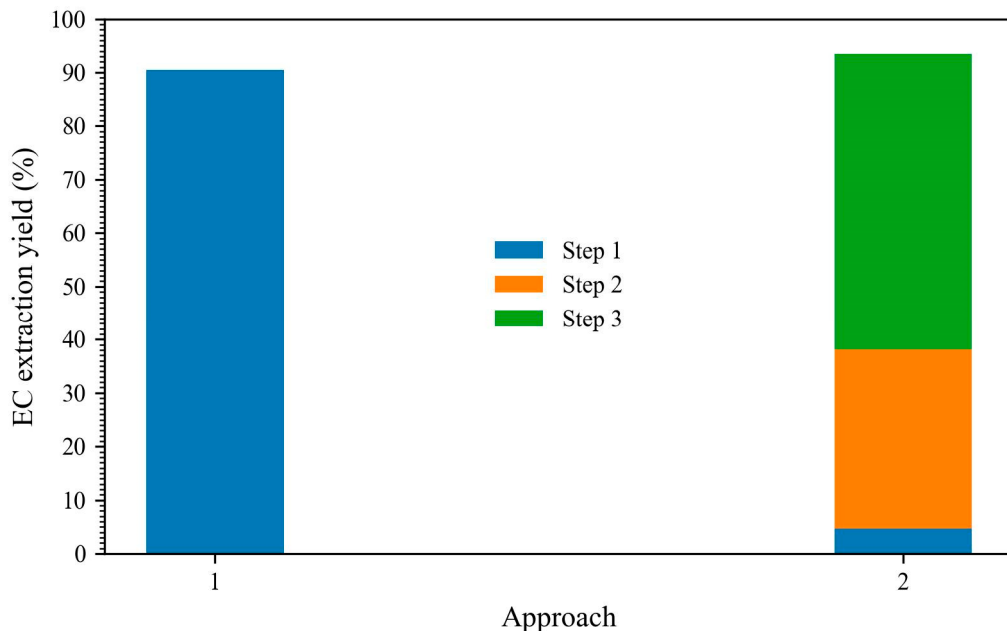


Figure 8. Extraction yield of EC from LiB black mass using two different extraction approaches. In the first approach, only 140 bar and 40 °C were used. In approach 2, the pressure was subsequently raised from 80 bar (Step 1) to 100 bar (Step 2) and then 140 bar (Step 3).

4. Conclusions

This study demonstrates the potential of scCO₂ as an effective solvent for EC extraction. The solubility of EC in scCO₂ increases from 0.24 g/kg of CO₂ to 8.4 g/kg of CO₂ by pressurizing within a range of 80 bar and 160 bar. The pressure range studied was below the cross-over pressure, meaning that the CO₂ density was the dominating factor governing EC dissolution. Importantly, the crystal structure, morphology, and chemical composition were mainly preserved after scCO₂ treatment, which confirms the non-destructive nature of the developed process for the sample.

The results imply that scCO₂ extraction can be implemented for the recycling of EC in a heterogeneous mixture of organics and inorganics such as Li-ion battery waste. A proof-of-concept experiment further validated the approach by successfully extracting EC from the Li-ion battery black mass, showcasing the potential of scCO₂ technology for practical recycling applications. Further research is required to study the mass-transfer characteristics during the extraction to increase the understanding of the process. This work paves the way for sustainable recycling solutions within the circular economy of battery electrolyte components.

Supplementary Materials: The following supporting information can be downloaded at: <https://www.mdpi.com/article/10.3390/batteries11030098/s1>, Figure S1: Cumulative collected EC (g) plotted against the CO₂ of the different experimental runs (denoted as I, II, and III) at (a) 80 bar, (b) 100 bar, (c) 120 bar, (d) 140 bar, (e) 160 bar and isothermal conditions at 60 °C; Table S1: Experimental vapor phase equilibrium data of propylene carbonate and CO₂ at various pressure and temperature conditions reported Hongling et al. and Rubin et al. [25,26].

Author Contributions: Conceptualization, N.Z. and B.E.; methodology, N.Z. and B.E.; software, N.Z. and C.C.; validation, N.Z.; formal analysis, N.Z.; investigation, N.Z. and C.C.; resources, B.E.; data curation, N.Z. and C.C.; writing—original draft preparation, N.Z.; writing—review and editing, B.E. and C.C.; visualization, N.Z.; supervision, B.E.; project administration, B.E.; funding acquisition, B.E. All authors have read and agreed to the published version of the manuscript.

Funding: This work was funded by the Swedish Energy Agency Battery Fund Program grant number P2019-90078, FORMAS—Swedish Research Council for Sustainable Development grant number 2021-01699, and Horizon Europe grant number Project 101069685—RHINOCEROS.

Data Availability Statement: The data presented in this study are available in the article and Supplementary Materials.

Acknowledgments: Funded by the European Union. Views and opinions expressed are however those of the author(s) only and do not necessarily reflect those of the European Union or European Climate, Infrastructure and Environment Executive Agency (CINEA). Neither the European Union nor the granting authority can be held responsible for them. The authors would like to acknowledge the Chalmers Material Analysis Laboratory, CMAL, for providing their facilities and assistance for the XRD and SEM characterization.

Conflicts of Interest: The authors declare no conflicts of interest.

References

1. Johnson, P.H. *Properties of Ethylene Carbonate and Its Use in Electrochemical Applications: A Literature Review*; University of California: Berkeley, CA, USA, 1985.
2. Environment International. Substance Evaluation Conclusion Document Evaluating Member State Competent Authority Year of Evaluation in CoRAP: 2018. 2019. Available online: <http://echa.europa.eu/regulations/reach/evaluation/substance-evaluation/community-rolling-action-plan> (accessed on 2 October 2024).
3. Xu, K. Nonaqueous liquid electrolytes for lithium-based rechargeable batteries. *Chem. Rev.* **2004**, *104*, 4303–4417. [[CrossRef](#)]
4. Ng, W.L.; Loy, A.C.M.; McManus, D.; Gupta, A.K.; Sarmah, A.K.; Bhattacharya, S. Exploring Greener Pathways and Catalytic Systems for Ethylene Carbonate Production. *ACS Sustain. Chem. Eng.* **2023**, *11*, 14287–14307. [[CrossRef](#)]
5. Niu, B.; Xu, Z.; Xiao, J.; Qin, Y. Recycling Hazardous and Valuable Electrolyte in Spent Lithium-Ion Batteries: Urgency, Progress, Challenge, and Viable Approach. *Chem. Rev.* **2023**, *123*, 8718–8735. [[CrossRef](#)] [[PubMed](#)]
6. Arshad, F.; Li, L.; Amin, K.; Fan, E.; Manurkar, N.; Ahmad, A.; Yang, J.; Wu, F.; Chen, R. A Comprehensive Review of Advancement in Recycling Anode and Electrolyte from Spent Lithium Ion Batteries. *ACS Sustain. Chem. Eng.* **2020**, *8*, 13527–13554. [[CrossRef](#)]
7. Nowak, S.; Winter, M. The role of sub- and supercritical CO₂ as “processing solvent” for the recycling and sample preparation of lithium ion battery electrolytes. *Molecules* **2017**, *22*, 403. [[CrossRef](#)] [[PubMed](#)]
8. Zhang, R.; Shi, X.; Esan, O.C.; An, L. Organic Electrolytes Recycling From Spent Lithium-Ion Batteries. *Glob. Chall.* **2022**, *6*, 2200050. [[CrossRef](#)]
9. Zhong, X.; Liu, W.; Han, J.; Jiao, F.; Qin, W.; Liu, T.; Zhao, C. Pyrolysis and physical separation for the recovery of spent LiFePO₄ batteries. *Waste Manag.* **2019**, *89*, 83–93. [[CrossRef](#)]
10. Zachmann, N.; Petranikova, M.; Ebin, B. Electrolyte recovery from spent Lithium-Ion batteries using a low temperature thermal treatment process. *J. Ind. Eng. Chem.* **2022**, *118*, 351–361. [[CrossRef](#)]
11. Knez, Ž.; Lütge, C. *Product, Process and Plant Design Using Subcritical and Supercritical Fluids for Industrial Application*; Springer: Berlin/Heidelberg, Germany, 2023; pp. 1–256. [[CrossRef](#)]
12. de Castro, M.D.L.; Valcárcel, M.; Tena, M.T. *Analytical Supercritical Fluid Extraction*; Springer: Berlin/Heidelberg, Germany, 1994. [[CrossRef](#)]
13. Vandenburg, H.J.; Clifford, A.A.; Bartle, K.D.; Carroll, J.; Newton, I.; Garden, L.M.; Dean, J.R.; Costley, C.T. Analytical extraction of additives from polymers. *Analyst* **1997**, *122*, 101R–116R. [[CrossRef](#)]
14. Zachmann, N.; Fox, R.V.; Petranikova, M.; Ebin, B. Implementation of a sub-and supercritical carbon dioxide process for the selective recycling of the electrolyte from spent Li-ion battery. *J. CO₂ Util.* **2024**, *81*, 102703. [[CrossRef](#)]
15. Grützke, M.; Mönnighoff, X.; Horsthemke, F.; Kraft, V.; Winter, M.; Nowak, S. Extraction of lithium-ion battery electrolytes with liquid and supercritical carbon dioxide and additional solvents. *RSC Adv.* **2015**, *5*, 43209–43217. [[CrossRef](#)]
16. Ingrosso, F.; Ruiz-López, M.F. Modeling Solvation in Supercritical CO₂. *ChemPhysChem* **2017**, *18*, 2560–2572. [[CrossRef](#)]
17. Altarsha, M.; Ingrosso, F.; Ruiz-Lopez, M.F. A New Glimpse into the CO₂-Philicity of Carbonyl Compounds. *ChemPhysChem* **2012**, *13*, 3397–3403. [[CrossRef](#)]

18. Huang, Z.; Shi, X.H.; Jiang, W.J. Theoretical models for supercritical fluid extraction. *J. Chromatogr. A.* **2012**, *1250*, 2–26. [[CrossRef](#)]
19. Abrahamsson, V.; Cunico, L.P.; Andersson, N.; Nilsson, B.; Turner, C. Multicomponent inverse modeling of supercritical fluid extraction of carotenoids, chlorophyll A, ergosterol and lipids from microalgae. *J. Supercrit. Fluids.* **2018**, *139*, 53–61. [[CrossRef](#)]
20. Anouti, M.; Dougassa, Y.R.; Tessier, C.; El Ouatani, L.; Jacquemin, J. Low pressure carbon dioxide solubility in pure electrolyte solvents for lithium-ion batteries as a function of temperature. *Meas. Predict.* **2012**, *50*, 71–79. [[CrossRef](#)]
21. Bartle, K.D.; Clifford, A.A.; Jafar, S.A.; Shilstone, G.F. Solubilities of Solids and Liquids of Low Volatility in Supercritical Carbon Dioxide. *J. Phys. Chem. Ref. Data.* **1991**, *20*, 713–756. [[CrossRef](#)]
22. Peschel, C.; van Wickeren, S.; Preibisch, Y.; Naber, V.; Werner, D.; Frankenstein, L.; Horsthemke, F.; Peuker, U.; Winter, M.; Nowak, S. Comprehensive Characterization of Shredded Lithium-Ion Battery Recycling Material. *Chem. A Eur. J.* **2022**, *28*, e202200485. [[CrossRef](#)]
23. NIST Chemistry WebBook—Thermophysical Properties of Fluid Systems, (n.d.). Available online: <https://webbook.nist.gov/chemistry/fluid/> (accessed on 3 October 2024).
24. Chrastil, J. Solubility of solids and liquids in supercritical gases. *J. Phys. Chem.* **1982**, *86*, 3016–3021. [[CrossRef](#)]
25. Hongling, L.; Rongjiao, Z.; Wei, X.; Yanfen, L.; Yongju, S.; Yiling, T. Vapor-liquid equilibrium data of the carbon dioxide + ethyl butyrate and carbon dioxide + propylene carbonate systems at pressures from (1.00 to 13.00) MPa and temperatures from (313.0 to 373.0) K. *J. Chem. Eng. Data.* **2011**, *56*, 1148–1157. [[CrossRef](#)]
26. Williams, L.L.; Mas, E.M.; Rubin, J.B. Vapor-liquid equilibrium in the carbon dioxide-propylene carbonate system at high pressures. *J. Chem. Eng. Data* **2002**, *47*, 282–285. [[CrossRef](#)]
27. MacEachern, L.; Kermanshahi-Pour, A.; Mirmehrabi, M. Supercritical carbon dioxide for pharmaceutical co-crystal production. *Cryst. Growth Des.* **2020**, *20*, 6226–6244. [[CrossRef](#)]
28. Martín, A.; Cocero, M.J. Micronization processes with supercritical fluids: Fundamentals and mechanisms. *Adv. Drug Deliv. Rev.* **2008**, *60*, 339–350. [[CrossRef](#)] [[PubMed](#)]
29. Markočić, E.K.; Leitgeb, M.; Primožič, M.; Hrnčić, M.K.; Škerget, M. Industrial applications of supercritical fluids: A review. *Energy* **2014**, *77*, 235–243. [[CrossRef](#)]
30. Yim, J.H.; Seo, W.W.; Jeon, J.S.; Lim, J.S.; Lee, J.W. Extraction of polyvinylidene fluoride binder materials for used secondary batteries using supercritical CO₂ for an effective battery recycling process. *J. Ind. Eng. Chem.* **2024**, *144*, 359–369. [[CrossRef](#)]

Disclaimer/Publisher’s Note: The statements, opinions and data contained in all publications are solely those of the individual author(s) and contributor(s) and not of MDPI and/or the editor(s). MDPI and/or the editor(s) disclaim responsibility for any injury to people or property resulting from any ideas, methods, instructions or products referred to in the content.